·Article ·

Advances in Polar Science

doi: 10.3724/SP.J.1085.2012.00163

September 2012 Vol. 23 No. 3: 163-169

Vertical structure of low-level atmosphere over the southeast Indian Ocean fronts

FENG Lin, LIU Lin*, GAO Libao & YU Weidong

Center for Ocean and Climate Research, First Institute of Oceanography, State Oceanic Administration, Qingdao 266061, China

Received 10 July 2012；accepted 30 August 2012

Abstract During the 25th Chinese National Antarctic Research Expedition, GPS radiosondes were launched to detect the atmospheric vertical structure over the southeast Indian Ocean frontal region. Some low-level characteristics along the cruise are studied based on in-situ observation. The observations reveal that vertical distributions of the low-level wind field and air temperature field on both sides of the Subantarctic Front are very different. A stronger (weaker) vertical gradient is on the cold (warm) side, which demonstrates that the mid-latitude ocean-atmosphere interaction is active in the southeast Indian Ocean frontal region. A low-level jet is observed over the Subantarctic Front, with speed up to 14 $m \cdot s^{-1}$. For the Antarctic polar front, low-level wind speed near the sea surface is greater than that aloft, in contrast with the situation of the Subantarctic Front. Comparing satellite remote sensing data and widely-used reanalysis datasets with our in-situ observations, differences of varying magnitudes are found. Air temperature from Atmospheric Infrared Sounder (AIRS) data has a limited difference. The European Center for Medium Range Weather Forecasts Interim Re-Analysis (ERA Interim) dataset is much more consistent with the observations than the National Centers for Environmental Prediction/National Center for Atmospheric Research (NCEP/NCAR) Reanalysis 1 in the southeast Indian Ocean frontal region.

Keywords **Subantarctic Front, Antarctic polar front, wind speed, air temperature**

Citation: Feng L, Liu L, Gao L B, et al. Vertical structure of low-level atmosphere over the southeast Indian Ocean fronts. Adv Polar Sci, 2012, 23: 163-169, doi: 10.3724/SP.J.1085.2012.00163

0 Introduction

Front is a common phenomenon in the global ocean. It is a narrow region where oceanic physical property such as temperature or salinity changes so sharply that the gradient across it is maximum. On both sides of a thermal front, sea surface temperature (SST) can modulate latent heat flux and sensible heat flux at the air-sea interface, and impact local atmospheric circulations above the front. The mid-latitude ocean-atmosphere interaction near the front is very different from that in the large-scale tropical region[1]. Observations show a significant negative correlation between SST and sea surface wind speed in the tropical ocean[2-5]. The warmer the SST, the weaker the sea surface wind and vice versa. This highlights the one-way effect of atmosphere on ocean, through changing ocean-atmospheric heat fluxes and the Ekman effect. However, SST has a significant positive correlation with sea surface wind in a strong frontal region, through vertical mixing induced by changes of static stability in the atmospheric boundary layer[1,6], high wind speed is likely to appear over warm SST region, whereas low wind speed is predominant over cold SST region[6-8]. Previous studies also indicate that on both sides of the front, changes of surface wind strength induced by SST always result in a linear relationship between surface wind vorticity or divergence fields and SST gradient[9-15].

Vertical shear associated with low-level wind speed near the front is considered to be the dominant cause of the positive correlation between SST and sea surface wind field[16-17]. Studies on the vertical structure of the low-level atmosphere over the front have clearly revealed the interaction between SST and sea surface wind[18-19].

There are various fronts broadly distributed in the

* Corresponding author (email: liul@fio.org.cn)

southern Indian Ocean[20-22]. Since these fronts are mainly in prevailing westerlies regions far from the continent, sparse *in situ* observations have been conducted[23-28], which hinders description and understanding of detailed vertical structures of the low-level atmosphere in the Southern Ocean. Actually, there is no systemic observation of fronts in the southeast part of the Indian Ocean by radiosonde as the conditions are so unfavorable. As a result, there are very few studies on fronts in this region, especially regarding vertical atmosphere structures above the front. With *in situ* data from radiosondes, launched during the 25th Chinese National Antarctic Research Expedition, we analyze the vertical structure of low-level wind and temperature fields over the southeast Indian Ocean fronts between Fremantle, Australia and the Chinese Antarctic Zhongshan Station.

1 Data and methods

1.1 *In situ* data

The R/V *XUE LONG* icebreaker left Fremantle for Zhongshan Station on 8 November 2008. The cruise crossing the southern Indian Ocean fronts lasted 8 days. During the voyage, we released 6 radiosondes across the Subantarctic Front and Antarctic polar front. The launched locations are shown in Figure 1, overlaid on the SST and sea surface wind field. The daily SST data are from the TRMM (Tropical Rainfall Measuring Mission) Microwave Imager (TMI), the first well-calibrated microwave radiometer capable of accurate through-cloud SST retrieval[29]. Its horizontal resolution is a quarter degree (~25 km). The sea surface winds are daily Quick Scatterometer (QuikSCAT) data[30]. We selected the background on 9 November to represent the entire voyage. The Subantarctic Front and the Antarctic polar front are determined according to certain criterias[25]. The boundary of the Subantarctic Front is where the maximum gradient of SST is between 5℃ and 9℃. For the other front, the criterion is that the northern terminus of the subsurface minimum temperature layer is bounded by the 2℃ isotherm in the 100—300 m layer. The result is that the two fronts are located at 45°S and 56°S, respectively.

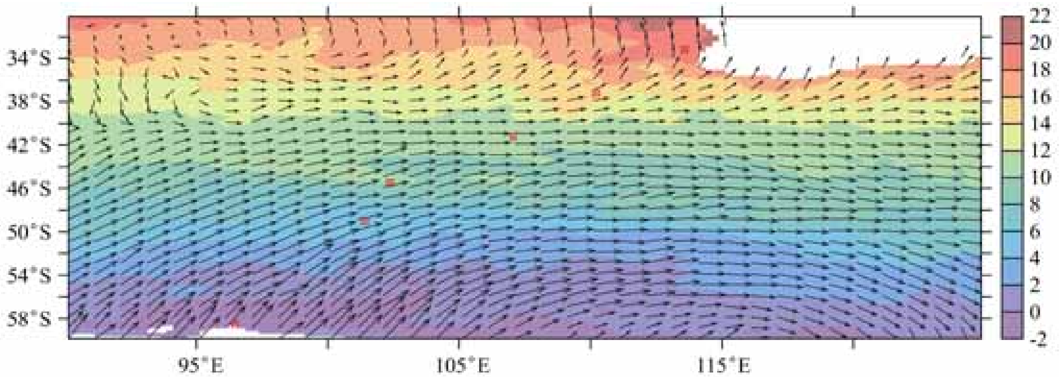

Figure 1 SST (shading, unit is °C) and sea surface wind (vectors, unit is $m \cdot s^{-1}$) in the southeast Indian Ocean on 9 November 2008. Small red boxes represent locations of radiosonde launches.

The radiosonde used in this expedition was the GPS low-level system produced by Lingheng Science and Technology Development Company (Beijing, China)[31]. Its receiver frequency is 407 MHz. GPS orientation technology replaced radar telemetry for measuring wind speed and direction, and a fast-response thermometer measured temperature. The vertical resolution was around 4 m per second for the experiment. Data were effectively transferred by data-transmission radio instead of an analog station. The equipment was tested in previous Antarctic and Arctic expeditions, proving its good stability for signal reception.

1.2 Reanalysis and satellite data

We select some widely-used datasets, including those from satellite remote sensing and reanalysis for cross calibrations. Daily air temperature data are the Atmospheric Infrared Sounder (AIRS) global 1.0°×1.0° product (http://disc.sci.gsfc.nasa.gov/giovanni/overview/index.html). The 4-times daily wind and air temperature data are from National Centers for Environmental Prediction/National Center for Atmospheric Research (NCEP/NCAR) Reanalysis 1[32] and European Centre for Medium Range Weather Forecasts (ECMWF) Interim Re-Analysis (ERA Interim)[33], respectively. All three datasets are interpolated onto the same grid as our observations for comparison.

2 Results and discussion

2.1 Vertical characteristics of the atmosphere over the southeast Indian Ocean fronts

The SST decreased from 20°C to −2°C along the cruise, and westerlies prevailed during the entire period (Figure 1). The vertical distribution of horizontal wind speed below 1 500 m is shown in Figure 2a. Obviously, there is a low-level strong flow over the Subantarctic Front, which is at about 250—350 m, with maximum speed reaching 18 $m \cdot s^{-1}$. This strong wind speed area, with speeds exceeding 16 $m \cdot s^{-1}$, stretches from 45°S to 48°S and occupies 80 m

(270—350 m) vertically. On either side of the front, the near-sea surface wind speed is much smaller than aloft. The wind speed increases with height, with a maximum larger than 20 $m \cdot s^{-1}$ at 1 300 m. This distribution is also found in middle levels (Figure 3a). However, vertical structures of wind speed on either side of the Subantarctic Front are not identical, especially at low levels. Below 400 m, the gradient on the cold side (48°—50°S) is stronger than that on the warm side (40°—42°S). The largest gradient is at a height of 150 m.

Around the Antarctic polar front (53°—59°S), the near-surface horizontal wind speed is stronger than that from 150 m to 1 000 m. Moreover, the vertical structure shows that wind speed increases northward throughout most of the low levels, which is very different from the symmetrical structure over the Subantarctic Front.

The vertical distribution of wind field over the Subantarctic Front is closely related to ocean-atmosphere interaction of the mid-latitudes. On the cold side of the Subantarctic Front, lower SSTs enhance the static stability of the overlying atmosphere, forming strong stratification near the sea surface and preventing downward energy transport from upper to lower levels. This results in weak wind speeds near the surface. Above 150 m, atmospheric stratification is not so strong and wind speed increases with the height. Based on our analysis, SST can affect vertical stratification of the low-level atmosphere (below 150 m) around the Subantarctic Front between Freemantle and Zhongshan Station. This is consistent with prior observations in the southeast Indian Ocean by Pezzi et al.[24]. The largest vertical gradient is at 150 m. This indicates that the mechanism that SST controlling low-level wind via modulation of atmospheric static stability is also applicable to mid-latitude weak fronts, where horizontal SST gradients are not so intensive.

Westerlies prevailed at the low levels, from Fremantle to the Zhongshan Station (Figure 2b). Vertical structure of zonal wind velocity is very similar to the horizontal wind speed pattern. For instance, it is roughly symmetrical about the Subantarctic Front. Even so, the details are different. The most significant feature is a jet stream emerging on the cold side of that front, whose center has speeds reaching 14 $m \cdot s^{-1}$ at 300 m. The jet extends over 500 km meridionally and 300 m vertically. At the same location on the warm side, there is a minimum area where the velocity is only 10 $m \cdot s^{-1}$. And the symmetric feature of the low-level vertical structure is broken off.

The meridional wind has a different vertical structure compared to either horizontal wind speed or zonal wind velocity (Figure 2c). The meridional wind below 200 m around the Subantarctic Front (40°—50°S) is controlled by northerlies. Above 200 m, the wind direction is opposite with maximum speed at 300 m, which generates the largest vertical gradient at 250 m. This region of strong southerlies is about 100 m in vertical direction and covers 200 km meridionally.

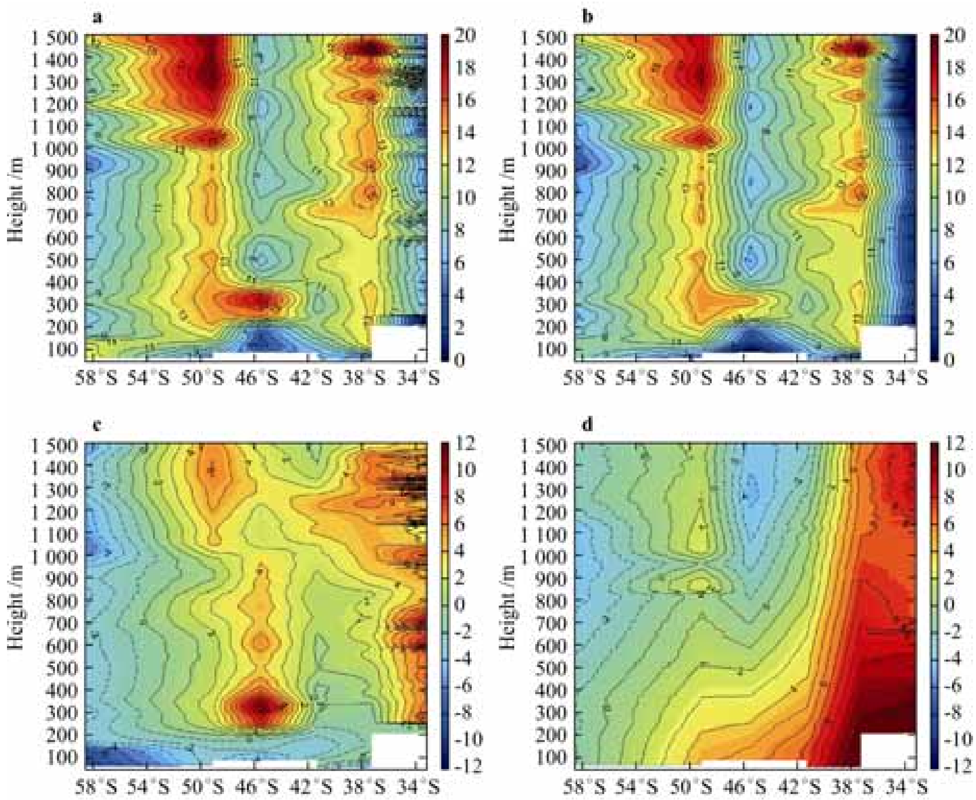

Figure 2 Latitude-height cross sections of horizontal wind speed (**a**), zonal wind velocity (**b**), meridional wind velocity (**c**), and air temperature (**d**) over the southeast Indian Ocean below 1500 m. Units of wind speed and temperature are $m \cdot s^{-1}$ and °C, respectively.

It is also the strongest meridional wind speed (>8 m·s^{-1}) region at low levels around the Subantarctic Front. Nevertheless, vertical structure above this front can still be considered symmetrical between 40° and 50°S, without regard to that above 1 000 m. Over the Antarctic polar front, southerlies are everywhere to form a barotropic distribution vertically. Wind speed near the sea surface is stronger than that in the upper levels, but its variation along height is modest. As the height enlarges, the south wind becomes strong. Overall, zonal wind is stronger than meridional wind over the southeast Indian Ocean fronts, making the low-level structure of wind speed primarily controlled by the distributions of zonal wind.

Figure 2d is the vertical distribution of air temperature. It shows that the vertical gradient is smaller on the warm side of the Subantarctic Front. In particular, the gradient is less than 0.01°C·m^{-1} and the isotherms are close to vertical at 40°S nearby. Over the cold side of the front, the vertical temperature gradient is greater. Correspondingly, the meridional gradient on the warm side is stronger than that on the cold side. Further, there is a cold gap 800 m above the front, which is more clearly depicted in Figure 3d. For higher mid levels, vertical structures of horizontal wind speed, zonal wind velocity, meridional wind velocity and air temperature are shown in Figure 3. Wind speed increases with height on both sides of the Subantarctic Front, and it is stronger on the cold side (Figure 3a and 3b). For meridional wind, the direction changes from about 2 700 m to higher levels at 37°S nearby (Figure 3c). The air temperature decreases at mid levels (Figure 3d).

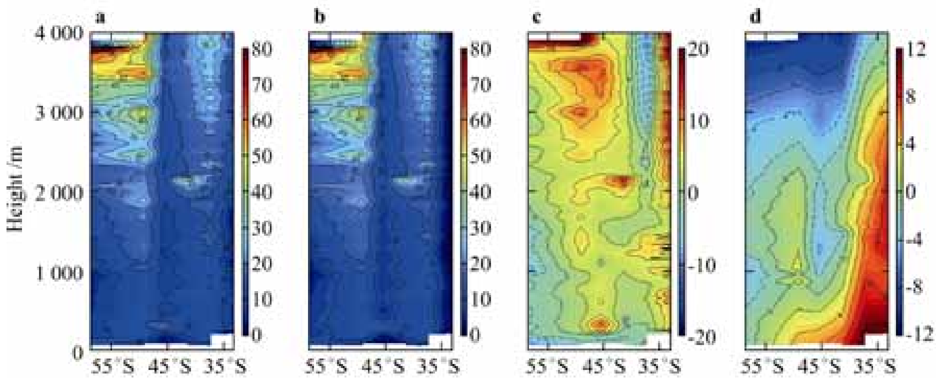

Figure 3 Latitude-height cross sections of horizontal wind speed (**a**), zonal wind velocity (**b**), meridional wind velocity (**c**), and air temperature (**d**) over the southeast Indian Ocean. Units of wind speed and temperature are m·s^{-1} and °C, respectively. And the vertical extent is up to 4 000 m.

2.2 Comparison to satellite and reanalysis datasets

Satellite remote sensing and reanalysis datasets are the dominant resources for research on the Southern Ocean due to a lack of *in situ* data. Naturally, a question should be answered. In the southern Indian Ocean, it remains a question as to which dataset is more reliable or gives smaller errors compared to *in situ* observations. We do a simple analysis on the satellite remote sensing data and the popular reanalysis datasets to investigate their differences between the observations preliminarily.

Compared to observations, AIRS temperature (Figure 4a) is able to capture the dominant features of the vertical structure presented by our radiosonde observation, though

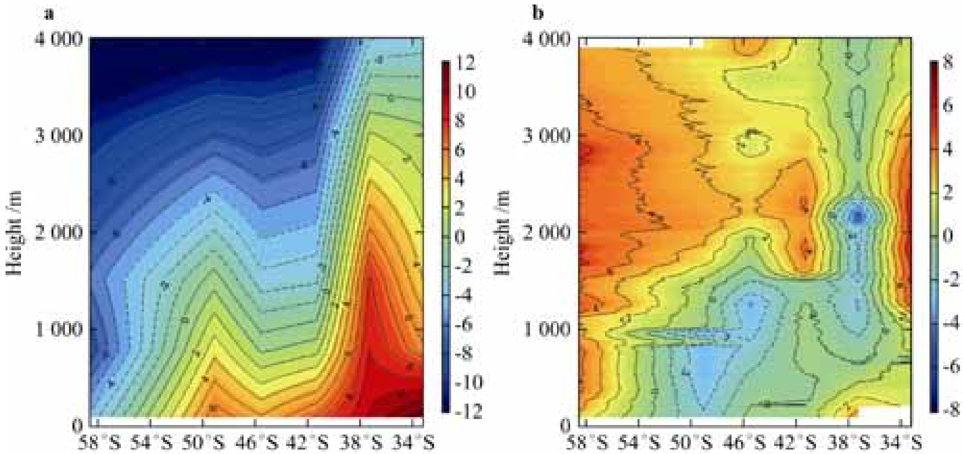

Figure 4 Latitude-height cross sections of air temperature from AIRS observation (**a**), and difference between radiosonde and AIRS observations (the former minus the latter) (**b**) over southeast Indian Ocean. Unit of temperature is °C.

not so detailed. Difference between AIRS and observation is shown in Figure 4b. The difference is smaller below 1 500 m. Observed data are colder than AIRS data on the cold side of the Subantarctic Front, and warmer over the Antarctic Front. The major difference is over the Antarctic Front.

The observations are also compared with NCEP/NCAR Reanalysis 1 and ERA Interim data. The difference with NCEP/NCAR Reanalysis 1 is remarkable, not only for values but also the spatial patterns (Figure 5). The situation seems not so poor at low levels, as the distribution of zonal and horizontal wind speed is somewhat symmetrical with the Subantarctic Front. Although the ERA Interim data cannot reproduce the mid-level jet stream between the two fronts either, its quality is much better according to the difference in Figure 6. This dataset captures the main features of the vertical structure, except in the near sea surface areas. For instance, the near-sea surface wind speed above the Antarctic polar front is smaller than aloft, and there are no northerlies over the Subantarctic Front. Among the four variables, air temperature has the smallest difference, and horizontal wind fields needs more improvements.

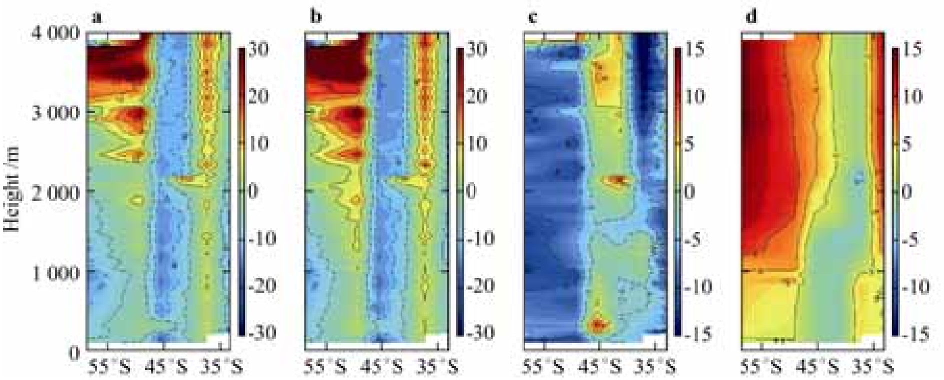

Figure 5 Latitude-height cross sections of differences in horizontal wind speed (**a**), zonal wind velocity (**b**), meridional wind velocity (**c**), and air temperature (**d**) between radiosonde observations and NCEP/NCAR Reanalysis 1, over southeast Indian Ocean. Units of wind speed and temperature are m·s^{-1} and °C, respectively.

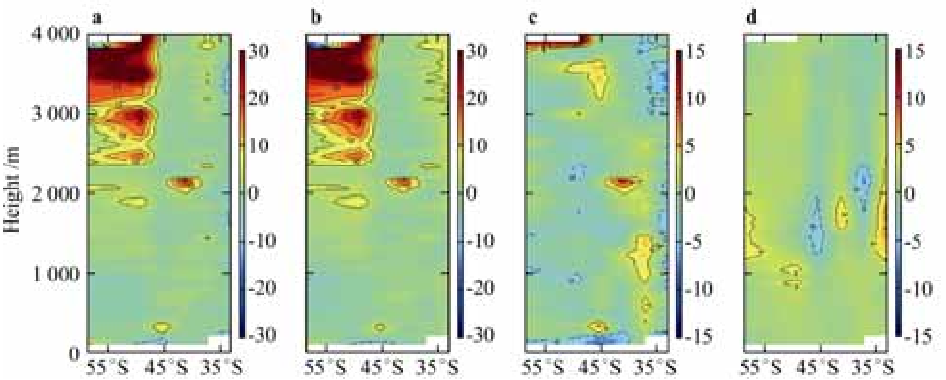

Figure 6 Latitude-height cross sections of differences in horizontal wind speed (**a**), zonal wind velocity (**b**), meridional wind velocity (**c**), and air temperature (**d**) between radiosonde observations and NCEP/NCAR Reanalysis 1, over southeast Indian Ocean. Units of wind speed and temperature are m·s^{-1} and °C, respectively.

3 Summary and conclusions

Based on *in situ* observations from radiosondes launched over the southeast Indian Ocean, vertical structure of the low-level atmosphere over oceanic fronts is described. The structures above the Subantarctic Front and the Antarctic polar front are different. At 250 m to 350 m above the former one, there is a region of strong wind with speed up to 14 m·s^{-1}, and westerlies make the major contribution. Vertical distributions of wind and air temperature on both sides of the Subantarctic front are not completely symmetrical, especially regarding the vertical gradient near the sea surface. There is a strong gradient on the cold side, and its maximum is around 150 m high. This proves that mid-latitude ocean-atmosphere interaction is still active in the southeast Indian Ocean frontal region. Wind direction has an obvious change at about 200 m, with northerlies near the sea surface and southerlies above. Wind speed increases with height. Over the Antarctic polar front, wind speed near the sea surface is greater than aloft.

Our observations are applied to validate AIRS data that its air temperature can depict the main features in low-level. Further, a comparison with two reanalysis dataset reveals that NCEP/NCAR Reanalysis 1 is not a wise choice for describing the vertical atmospheric structure in this frontal region; ERA Interim is much better though it has some deficiencies at the near sea surface levels.

This study demonstrates that the positive relationship between SST across oceanic fronts and low-level wind speed, which has been observed over numerous mid-latitude oceanic fronts[7-8,13], also holds in the southern Indian Ocean. The mechanism responsible for this relationship has been presented in previous studies[7-8]. On the other hand, the response of higher atmosphere to SST around the front is quasi-barotropic, which is similar to the phenomena observed in the Kuroshio Current region[13]. In contrast to the strong frontal region in the eastern Pacific Ocean, the frontal region in the southeast Indian Ocean is wider, the SST gradient weaker, and the fronts more dispersed. Therefore, more observations are needed to confirm whether our findings are peculiar to weak fronts. There are further limitations to this study. First, only six radiosondes were launched, which is inadequate for depicting detailed horizontal structures of atmosphere. Second, the radiosonde does not have a humidity sensor and humidity data are unavailable for diagnosis. In the very near future, we will conduct more *in situ* experiments using multi-function radiosondes. These will help us examine detailed frontal structures over the southern Indian Ocean, to verify the findings herein.

Acknowledgements We thank all the crews of the 25th Chinese National Antarctic Research Expedition for their great supports. This work is supported by the National Program on Key Basic Program, Research Program of China (973 Program, Grant nos. 2010CB950304 and 2012CB955601), SOA Science Fund for Young Scholars (Grant no. 2011244), the Chinese Polar Strategy Fund (Grant no. 20072017), the Chinese Polar Investigation Fund (Grant no. CHINARE 2012-01-01), and the International Cooperation Fund (Grant no. JD201002).

References

1 Xie S P. Satellite observations of cool ocean-atmosphere interaction. Bull Amer Meteor Soc, 2004, 85(2): 195-208.

2 Mantua N J, Hare S R, Zhang Y, et al. A Pacific interdecadal climate oscillation with impacts on salmon production. Bull Amer Meteor Soc, 1997, 78(6): 1069-1079.

3 Okumura Y, Xie S P, Numaguti A, et al. Tropical Atlantic air-sea interaction and its influence on the NAO. Geophys Res Lett, 2001, 28(8): 1507-1510.

4 Tomita T, Xie S P, Nonaka M. Estimates of surface and subsurface forcing for decadal sea surface temperature variability in the mid-latitude North Pacific. J Meteor Soc Japan, 2002, 80(5): 1289-1300.

5 Visbeck M, Chassignet E P, Curry R G, et al. The ocean's response to North Atlantic Oscillation variability// Hurrell J W, Kushnir Y, Ottersen G, et al. The North Atlantic Oscillation: Climatic Significance and Environmental Impact. Geophysical Monograph Series, 2003, 134: 113-145.

6 Chelton D B, Michael G S, Michael H F, et al. Satellite measurements reveal persistent small-scale features in ocean winds. Science, 2004, 303(5660): 978-983.

7 Xie S P, Ishiwatari M, Hashizume H, et al. Coupled ocean-atmosphere waves on the equatorial front. Geophys Res Lett, 1998, 25(20): 3863-3866.

8 Chelton D B, Esbensen S K, Schlax M G, et al. Observation of coupling between surface wind stress and sea surface temperature in the eastern tropical Pacific. J Climate, 2001, 14(7): 1479-1498.

9 Deser C, Wahl S, Bates J J. The influence of sea surface temperature on stratiform cloudiness along the equatorial front in the Pacific Ocean. J Climate, 1993, 6(6): 1172-1180.

10 Hashizume H, Xie S P, Liu W T, et al. Local and remote atmospheric response to tropical instability waves: A global view from space. J Geophys Res, 2001, 106(D10): 10173-10185.

11 Thum N, Esbensen S K, Chelton D B, et al. Air-sea heat exchange along the northern sea surface temperature front in the eastern tropical Pacific. J Climate, 2002, 15(23): 3361-3378.

12 Nonaka M, Xie S P. Covariations of sea surface temperature and wind over the Kuroshio and its extension: Evidence for ocean-to-atmospheric feedback. J Climate, 2003, 16(9): 1404-1413.

13 Xu H M, Wang L W, He J H. Observed oceanic feedback to the atmosphere over the Kuroshio Extension during spring time and its possible mechanism. Chinese Science Bulletin, 2008, 53(12): 1905-1912.

14 White W B, Annis J L. Coupling of extratropical mesoscale eddies in the ocean to westerly winds in the atmospheric boundary layer. J Phys Oceanogr, 2003, 33(5): 1095-1107.

15 O'Neill L W, Chelton D B, Esbensen S K. Observations of SST-induced perturbations of the wind stress field over the Southern Ocean on seasonal timescales. J Climate, 2003, 16(14): 2340-2354.

16 Hayes S P, McPhaden M J, Wallace J M. The influence of sea surface temperature on surface wind in the eastern equatorial Pacific. J Climate, 1989, 2(12): 1500-1506.

17 Wallace J M, Mitchell T P, Deser C. The influence of sea surface temperature on surface wind in the eastern equatorial Pacific: Seasonal and interannual variability. J Climate, 1989, 2(12): 1492-1499.

18 Vecchi G A, Xie S P, Fischer A S. Ocean-atmosphere covariability in the Western Arabian Sea. J Climate, 2004, 17(6): 1213-1224.

19 Park K A, Cornillon P C. Stability-induced modification of sea surface winds over Gulf Stream rings. Geophys Res Lett, 2002, 29(24), 2211, doi: 101029/ 2001GL014236.

20 Kostianoy A G, Ginzburg A I, Frankignoulle M, et al. Fronts in the Southern Indian Ocean as inferred from satellite sea surface temperature data. Journal of Marine Systems, 2004, 45(1-2): 55-73.

21 He Z G, Dong Z Q, Hu J Y. Upper ocean hydrographic properties of southeast Indian Ocean in Austral Summer, 2003. Chinese Journal of Polar Research, 2003, 15(3): 195-206 (in Chinese).

22 Xu S Q, Chen L Q, Implication for estimate air-sea CO_2 fluxes in the Southern Ocean based on satellite data and In situ investigations. Chinese Journal of Polar Research, 2007, 19(2): 151-157 (in Chinese).

23 Sun H, Gao Z Y. Advances in the study of air-sea CO_2 fluxes in the Southern Ocean. Chinese Journal of Polar Research, 2009, 21(1): 60-68 (in Chinese).

24 Pezzi L P, Souza R B, Dourado M S, et al. Ocean-atmosphere in situ observations at the Brazil-Malvinas Confluence region. Geophys Res Lett, 2005, 32(22): L22603, doi: 101029/2005GL023866.

25 Gao G P, Han S Z, Dong Z Q, et al. Structure and variability of fronts in the South Indian Ocean along sections from Zhongshan Station to Fremantle. Acta Oceanologica Sinica, 2003, 25(6): 9-19 (in Chinese with English abstract).

26 Shi J X, Zhao J P. Advances in Chinese studies on water masses, circulation and sea ice in the Southern Ocean (1995-2002). Advances in Marine Science, 2002, 20(4): 116-126 (in Chinese).

27 Shi M C, Miao Y T, Yu H H, et al. The summer frontal zonal at 110°E in the South Indian Ocean and its variability. Periodical of Ocean University of China, 1995, 25(Sup.): 394-405 (in Chinese).

28 Gao G P, Liu Q, Shi M C. Location of the Antarctic polar front in the Indian Ocean and the separation of sinking Antarctic surface water. Periodical of Ocean University of China, 1995, 25(Sup.): 424-431 (in Chinese).

29 Wentz F J, Gentemann C, Smith D, et al. Satellite measurements of sea surface temperature through clouds. Science, 2000, 288(5467): 847-850.

30 Callahan P S, Lungu T. QuikSCAT Science Data Product User's Manual (v30). Jet Propul Lab, 2006.

31 Lv W T. A multi-function and high resolution GPS radiosonde system. Chinese Academy of Meteorological Sciences Annual Report, 2006, 1: 31-31.

32 Kalnay E, Kanamitsu M, Kistler R, et al. The NCEP/NCAR 40-year reanalysis project. Bull Amer Meteor Soc, 1996, 77(3): 437-470.

33 Dee D P, Uppala S M, Simmons A J, et al. The ERA-Interim reanalysis: configuration and performance of the data assimilation system. Quart J Roy Meteor Soc, 2011, 137(656): 553-597.